Widespread and precise reprogramming of yeast protein–genome interactions in response to heat shock

Vinesh Vinayachandran,[1,2] Rohit Reja,[1,3] Matthew J. Rossi,[1] Bongsoo Park,[1,2] Lila Rieber,[1] Chitvan Mittal,[1] Shaun Mahony,[1] and B. Franklin Pugh[1]

[1] *Center for Eukaryotic Gene Regulation, Department of Biochemistry and Molecular Biology, Pennsylvania State University, University Park, Pennsylvania 16802, USA*

Gene expression is controlled by a variety of proteins that interact with the genome. Their precise organization and mechanism of action at every promoter remains to be worked out. To better understand the physical interplay among genome-interacting proteins, we examined the temporal binding of a functionally diverse subset of these proteins: nucleosomes (H3), H2AZ (Htz1), SWR (Swr1), RSC (Rsc1, Rsc3, Rsc58, Rsc6, Rsc9, Sth1), SAGA (Spt3, Spt7, Ubp8, Sgf11), Hsf1, TFIID (Spt15/TBP and Taf1), TFIIB (Sua7), TFIIH (Ssl2), FACT (Spt16), Pol II (Rpb3), and Pol II carboxyl-terminal domain (CTD) phosphorylation at serines 2, 5, and 7. They were examined under normal and acute heat shock conditions, using the ultrahigh resolution genome-wide ChIP-exo assay in *Saccharomyces cerevisiae*. Our findings reveal a precise positional organization of proteins bound at most genes, some of which rapidly reorganize within minutes of heat shock. This includes more precise positional transitions of Pol II CTD phosphorylation along the 5′ ends of genes than previously seen. Reorganization upon heat shock includes colocalization of SAGA with promoter-bound Hsf1, a change in RSC subunit enrichment from gene bodies to promoters, and Pol II accumulation within promoter/+1 nucleosome regions. Most of these events are widespread and not necessarily coupled to changes in gene expression. Together, these findings reveal protein–genome interactions that are robustly reprogrammed in precise and uniform ways far beyond what is elicited by changes in gene expression.

[Supplemental material is available for this article.]

A wide variety of proteins assemble onto DNA to regulate and elicit gene expression. Knowledge of their positional organization provides insight into common mechanisms of genome-wide regulation. Further insight may be gained by observing their redistribution when the genome is reprogrammed by environmental signals. While it is expected that reorganization of proteins involved in transcription and chromatin may be largely restricted to genes that are undergoing changes in expression, there may be reorganization events that are not overtly tied to changes in gene expression (Zanton and Pugh 2006; Weiner et al. 2012).

Acute heat shock has been a model system to de-construct gene regulatory mechanisms in the budding yeast *Saccharomyces cerevisiae* because it can be applied instantaneously (Gasch et al. 2000; Causton et al. 2001; Chen and Hahn 2004; Zanton and Pugh 2006; Venters et al. 2011; Anandhakumar et al. 2016). This ensures that genome-reprogramming events occurring within minutes are a direct consequence of environmental sensing. Other events, such as gene expression changes occurring through the cell cycle and in response to heat shock, occur over much longer periods of time and do not influence events occurring within a few minutes of heat shock.

The heat shock response is a vital evolutionarily conserved reprogramming system that is designed to induce expression of cytoprotective genes as well as meet altered energy demands (Gasch et al. 2000; Verghese et al. 2012). It may also serve to prepare cells for likely encounters with additional near-term stress (Zanton and Pugh 2006; Berry and Gasch 2008). About 300 genes are induced and another 600 repressed by heat shock (Gasch et al. 2000; Causton et al. 2001). Heat shock-induced genes appear to be variously regulated since not all are bound by the sequence-specific activator Hsf1 (Chen and Hahn 2004), and thus there may not be a single response mechanism (de Jonge et al. 2017). The focus of the work here is on genome-reprogramming events as a means to understand gene regulatory mechanisms.

Prior genome-wide approaches have examined a wide range of factors involved in the heat shock response (Hahn et al. 2004; Zanton and Pugh 2004; Shivaswamy and Iyer 2008; Shivaswamy et al. 2008; Venters and Pugh 2009; Ghosh and Pugh 2011; Venters et al. 2011; Anandhakumar et al. 2016). However, the technology at the time was low resolution, thereby allowing only the general organization of the highest confidence binding events to be identified. Consequently, this has provided only a part of the regulatory picture. Improved spatial resolution of genome-wide assays like ChIP-exo have led to dramatic improvements in deciphering genome-wide mechanisms (Rhee and Pugh 2011), by revealing the positional organization of factors.

Present addresses: [2]Department of Environmental Health and Engineering, Johns Hopkins Bloomberg School of Public Health, Baltimore, MD 21205, USA; [3]Astrix Software Technology, Inc., Red Bank, NJ 07701, USA
Corresponding author: bfp2@psu.edu
Article published online before print. Article, supplemental material, and publication date are at http://www.genome.org/cgi/doi/10.1101/gr.226761.117.

ChIP-exo utilizes a 5′-3′ exonuclease to degrade one strand of DNA up to the point where it is blocked by a protein-DNA crosslink produced in vivo with formaldehyde. Formaldehyde crosslinking preserves precise in vivo binding locations (within a few base pairs), and ChIP-exo allows their positional organization within complexes to be resolved. Importantly, if that organization changes in response to signaling events, including structural reorganization, these events may be captured by changes in crosslinking patterns and monitored on a genomic scale. Since formaldehyde reacts rapidly, high temporal resolution is achieved, for example, in response to the instantaneous exposure to nonlethal heat stress. Thus, temporal and spatial organization of regulatory events in a genome is visible in the ChIP-exo assay.

The types of genes that respond to acute heat shock are typically in the highly regulated SAGA-dominated class (Venters et al. 2011). SAGA-dominated genes, representing ~10%–20% of the yeast genome, are defined as having mRNA expression levels that display a greater dependence on SAGA compared to the rest of the genome (Kuras et al. 2000; Lee et al. 2000; Huisinga and Pugh 2004). All other genes are in the TFIID-dominated class, reflecting relatively greater dependency on TFIID than on SAGA. Importantly, both classes are inter-dependent on SAGA and TFIID (Huisinga and Pugh 2004; Ghosh and Pugh 2011), with the difference being a matter of degree or timing.

Here, we used ChIP-exo to examine the genome-wide structural organization of a subset of genome regulatory factors in budding yeast in response to rapid reprogramming by acute heat shock. Factors include a variety of the general transcription factors (GTFs) that had previously been examined under non-heat shock conditions (Rhee and Pugh 2012), but not under heat shock. We also examined chromatin regulatory factors and Hsf1. Beyond the ~10%–15% of the yeast genome that changes gene expression upon heat shock, we examined the genome stratified by general RNA or gene classes such as noncoding (SUTs, CUTs, XUTs), TFIID- vs. SAGA-dominated, or ribosomal protein (RP) encoding. RP genes represent a large cohort of 137 similarly regulated heat shock-repressed genes (Reja et al. 2015).

Results

Genome-wide factor binding is reprogrammed within 3 min of heat shock

This study examined four parameters relevant to factor organization broadly across the yeast genome: protein factors, binding time course, gene classes, and positioning within genes. Factors include the following (ChIP targeted subunit indicated in parentheses): nucleosomes (H3), H2AZ (Htz1), SWR (Swr1), RSC (Rsc1, Rsc3, Rsc58, Rsc6, Rsc9, Sth1), SAGA (Spt3, Spt7, Ubp8, Sgf11), Hsf1, TFIID (Spt15 and Taf1), TFIIB (Sua7), TFIIH (Ssl2), FACT (Spt16), and Pol II (Rpb3 and CTD serine 2, 5, and 7 phosphorylation).

We initially explored temporal conditions of rapid genomic reprogramming (0, 3, 6, 9, 12, 15 min of 37°C heat shock) of a subset of factors so as to examine the dynamic reorganization of these factors. ChIP-exo data were of high quality, based on the high concordance between biological replicates (e.g., TFIIH [Ssl2] in Supplemental Fig. S1A) and with mRNA expression (Supplemental Fig. S1B,C). However, for lowly transcribed genes, a wide range of mRNA levels was associated with a relatively narrow range of occupancy, which likely reflects post-recruitment mechanisms that control mRNA levels.

Figure 1 shows the strand-separated ChIP-exo patterning (reflecting structural interactions of each factor with sense versus antisense DNA) at three representative genes of this study, including those that are induced, repressed, or largely unchanged upon 3 min of heat shock (and lowly expressed). This offers a view of the rawest form of the data. What is clear beyond expected occupancy changes is the well-resolved positional organization of

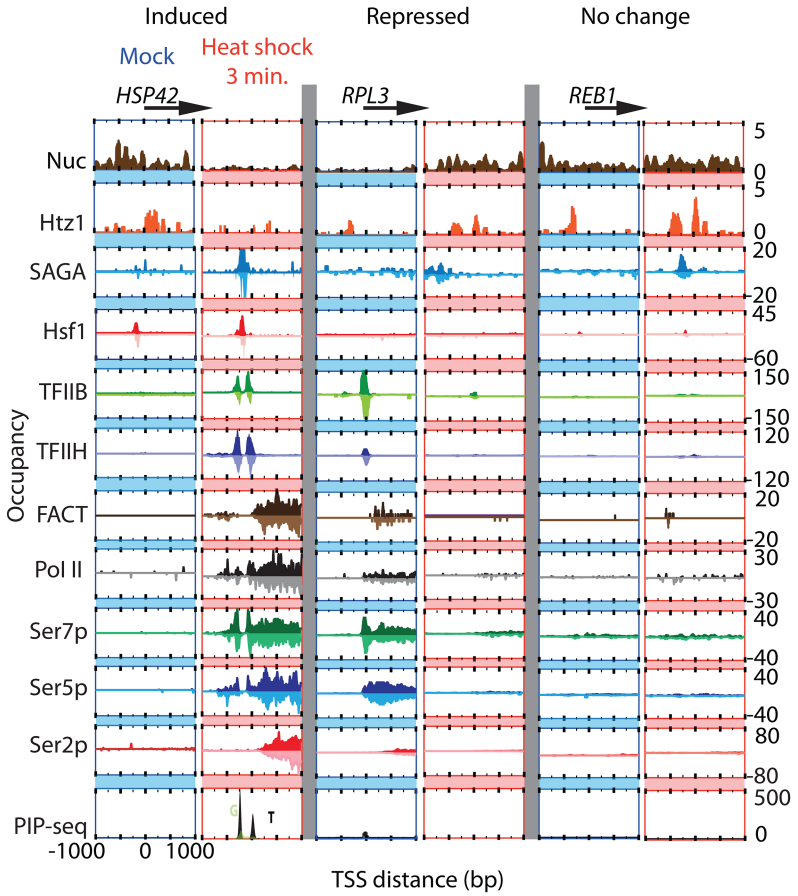

Figure 1. Factor occupancy at three genes before and after heat shock. Smoothed distribution of unshifted ChIP-exo tag 5′ ends (exonuclease stop sites) on forward and reverse strands (with the latter being inverted) on induced *HSP42*, repressed *RPL3*, and housekeeping *REB1* genes upon mock or after 3 min of heat shock. Nucleosomes (Nuc) represent fragment midpoints of MNase-digested H3-immunoprecipitated chromatin. All TSSs are oriented such that the direction of transcription is to the *right*. The *bottom* panel of each column corresponds to melted PIC DNA derived from TFIIB PIP-seq. Foreground "T" nucleotides are in black and background "G" nucleotides are in green. *Y*-axes are scaled for each factor to fit the frame and are all on the same scale for a particular factor (row).

individual factors along the DNA. For example, bidirectional transcription is evident at the *HSP42* promoter, that includes two preinitiation complexes (PICs) ~250 bp apart, with sequence-specific Hsf1 and SAGA inter-digitated between the two. The divergent upstream transcription is relatively short.

The occupancy level and positional organization of factors and their reorganization dynamics during acute heat shock were analyzed separately for six classes of Pol II transcription units: (1) the coordinately regulated and stress-repressible ribosomal protein genes; (2) all mRNA genes of the SAGA-dominated class, many of which tend to be stress-induced and utilize complex chromatin-based repression mechanisms; (3) all mRNA genes of the TFIID-dominated class, which tend to play housekeeping roles and have constitutive nucleosome-free promoters regions (NFR); and (4–6) CUTs, SUTs, and XUTs, representing unstable, stable, and Xrn-regulated noncoding transcription units, respectively.

The GTFs, as represented by TFIIH (Ssl2), were lost rapidly (<3 min after heat shock) at RP genes (Supplemental Fig. S2, left panels), whereas at the class of TFIID-dominated genes and at noncoding transcription units, there was a gradual decline to a new steady state over a 15-min period. In contrast, at the class of SAGA-dominated genes, there was a burst of TFIIH (Ssl2) binding, followed by a gradual decline to a new steady state. When the SAGA (Spt3) complex was examined (Supplemental Fig. S2, right panels), it followed the general trend of TFIIH (Ssl2). There was a burst of SAGA binding in all gene classes except RP, followed by a gradual loss. SAGA was already at RP genes and rapidly dissociated upon heat shock. Its function at RP genes is distinct from SAGA-dominated genes (Downey et al. 2013). The magnitude of the composite effects reported in these plots is certainly muted by gene-class averaging, for which only a fraction of genes is actually changing in occupancy and a portion may be changing in directions opposite to the overall trend. Composite (gene-average) plots of more factors (Spt3, Spt15, Sua7, Taf1, Ssl2, Rpb3, and Hsf1), separated into three classes (induced, repressed, or no change upon heat shock), showed rapid kinetics, where maximum binding at induced genes and maximum loss at repressed genes was achieved by 3 min of heat shock (Supplemental Fig. S3A, B). These results allowed us to focus our data collection on the 3-min time point, so as to monitor peak responses that were qualitatively the same at other slightly longer time points.

Many aspects of heat shock-induced factor reorganization are not gene-selective

We first examined factor binding to the entire genome, so as to provide an important global context for more zoomed-in analyses. To represent the entire genome, transcription units were plotted as single-dimensional tracks in a heat map. Tracks were aligned by transcription unit midpoint (start to end, TSS-TES) and sorted by unit length within each class (Fig. 2). Several novel observations were made, along with confirmation of prior findings. First, factors had very specific canonical locations relative to the start and end of transcription (left vs. right edge of each "bell" in Fig. 2 were distinct regardless of gene length), confirming that there is a precise and recurring organizational theme to factor assembly. This was not observed with the BY4741 negative control (No tag).

Second, the vast majority of promoters (~90%) had precisely-positioned GTFs before and after heat shock (Fig. 3), which is a novel observation. They were also constitutively nucleosome-free in accordance with prior work (Shivaswamy et al. 2008). This indicates that, during rapid growth and acute heat shock, the vast majority of all promoters retain a precisely positioned PIC within a constitutive NFR, even if the PIC is at low levels. NFR width correlated with PIC occupancy, ranging from ~150 bp (nucleosome edge-to-edge) at high occupancy to ~100 bp at low occupancy

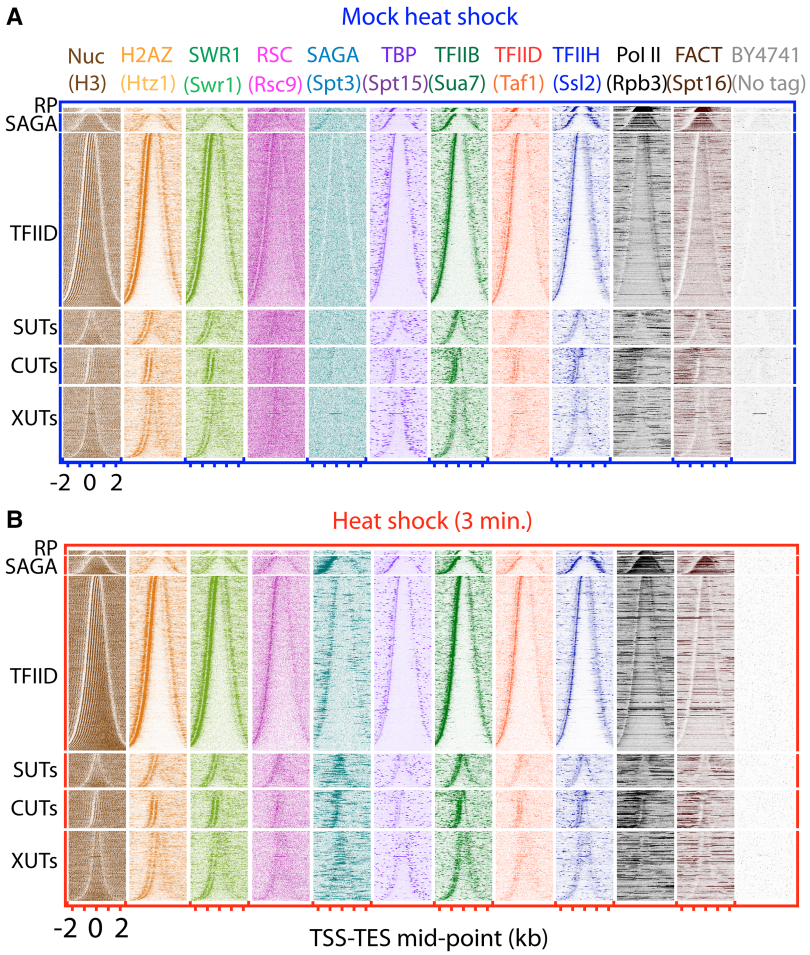

Figure 2. Factor occupancy at all genes before and after heat shock. (*A*) Yeast cultures were either mock-treated (*upper* set of panels) or (*B*) heat shocked (*lower*) for 3 min at 37°C. ChIP-exo tag 5′ ends were plotted relative to transcription unit midpoints (start to end from *left* to *right*). Rows are sorted by unit length and grouped by class: ribosomal protein genes (RP, $n = 130$), SAGA-dominated genes (SAGA, $n = 451$), TFIID-dominated genes (TFIID, $n = 4260$), and noncoding SUTs ($n = 846$), CUTs ($n = 924$), and XUTs ($n = 1720$). All rows across data sets are linked.

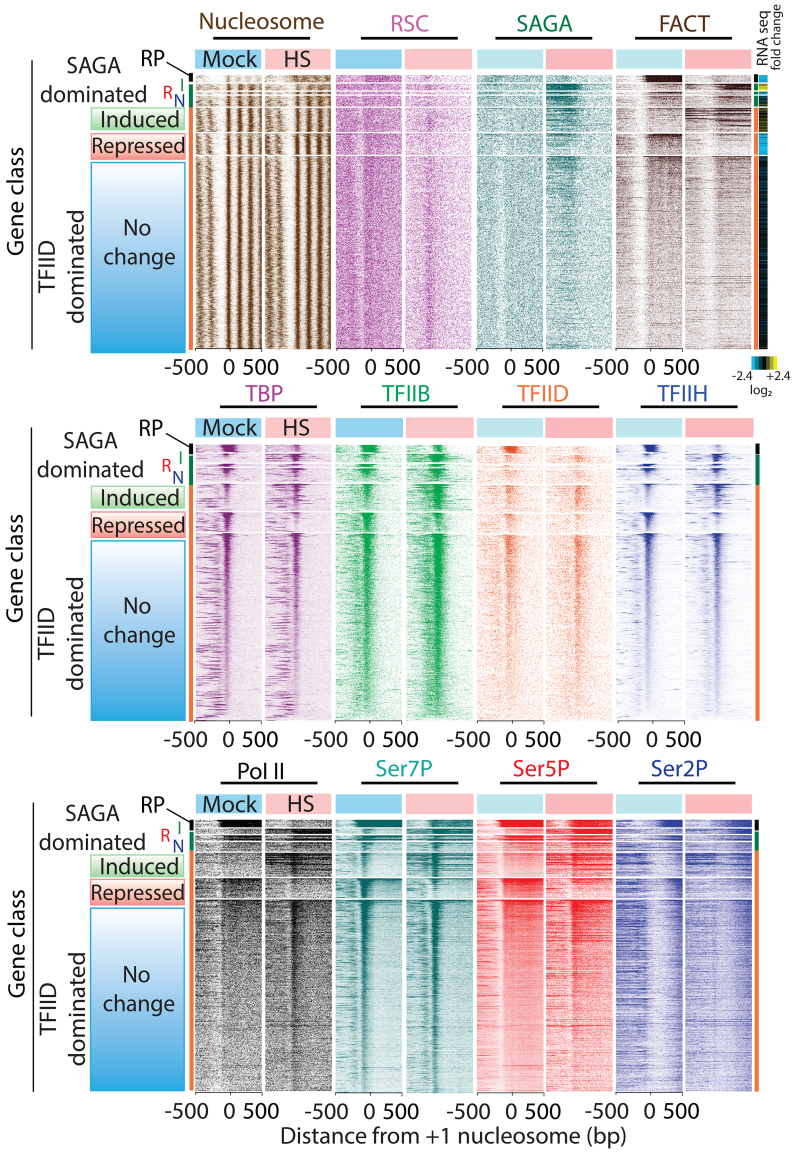

Figure 3. Segregated and sorted heat shock response. ChIP-exo tag 5′ ends were plotted from ±500 bp relative to +1 nucleosome dyads, panel-separated based on mock or 3 min of heat shock, segregated by gene class (RP, SAGA, TFIID) and then by increased/induced (I), decreased/repressed (R), or no changes (N) in TFIIH (Ssl2) occupancy upon heat shock: SAGA-dominated genes (I,R,N, $n = 160$, 55, 252, respectively), TFIID-dominated genes (I,R,N, $n = 488$, 353, 3358, respectively). Within each segregated group, rows were sorted by TFIIH occupancy in the region 100 bp upstream of to 100 bp downstream from the TSS. Also shown in the far *upper right* is a heat map of $\log_2$ fold-changes in mRNA expression after 15 min of heat shock, using data from Yassour et al. (2009).

(Fig. 3, nucleosomes, and Supplemental Fig. S4), which is consistent with prior reports (Radman-Livaja and Rando 2010; Weiner et al. 2010; Jansen et al. 2012).

Third, at most genes, occupancy levels of most factors changed little upon acute and sustained heat shock (Fig. 3; Supplemental Fig. S3A). This is consistent with only ~10%–15% of the genome changing mRNA expression (Fig. 3, mRNA). As expected, substantial loss of GTFs occurred at RP genes (Supplemental Fig. S3B; Reja et al. 2015). Heat shock-induced genes, as defined by an increase in TFIIH (Ssl2), were proportionally more in the stress-induced SAGA-dominated class than in the TFIID-dominated class (2.5× random chance) (Huisinga and Pugh 2004). The PIC occupancy at SAGA-dominated genes was also induced to a greater magnitude than TFIID-dominated genes. Fourth, upon heat shock, RSC (Rsc9) had widespread alterations in its positional organization (Fig. 2). Similar trends did not occur with PIC assembly and nucleosome organization (Fig. 3). Like RSC, but in contrast to the GTFs, there was a major reorganization of SAGA, FACT, and Pol II occupancy and/or positioning upon heat shock, not all of which were tied to changes in expression. We next expand on these novel observations.

Hsf1 and SAGA (Spt3) are precisely copositioned

Under normal conditions, SAGA (Spt3) was largely absent from most genes (Fig. 3, "Spt3" mock heat shock). However, binding was detected at normally active SAGA-dominated genes. In contrast, TFIID (Taf1) was detected at most genes but was relatively depleted at SAGA-dominated genes. As a control comparison, GTFs were not depleted at SAGA-dominated genes. These findings do not agree with a study published while this work was under review (Baptista et al. 2017). Since two fundamentally different assays were used (ChEC-seq versus ChIP-exo), a detailed comparison of the two approaches is warranted.

SAGA (Spt3) binding increased dramatically upon 3 min of heat shock at many promoter regions within all transcription classes, particularly at induced SAGA-dominated genes as expected of this class. SAGA (Spt3) also increased at many CUTs and at TFIID-dominated genes (Fig. 2), including those that became repressed. Our findings were verified with other SAGA subunits, including Spt7, Ubp8 and Sgf11, that were unique to SAGA (Supplemental Fig. S5A). The binding of SAGA (Spt3) appeared more gene-selective than what was seen for GTFs but correlated with gene activity. The heat shock-induced recruitment of SAGA to TFIID-dominated genes is noteworthy in that this gene class tends to be less dependent on SAGA during heat shock. Indeed, their mRNA expression was not particularly sensitive to deletion of *SPT3* (Fig. 4A, left vs. right set of bars), in contrast to the corresponding Spt3-bound SAGA-dominated genes.

MEME (Bailey and Elkan 1994) analysis of heat shock-induced SAGA-bound regions revealed specific enrichment of Hsf1 binding sites. We therefore mapped Hsf1 by ChIP-exo. Hsf1 was constitutively bound to these sites, as expected from historical single-gene studies (Jakobsen and Pelham 1988). Heat shock also caused increased Hsf1 binding, as previously reported (Hahn et al. 2004). The composite peak of SAGA (Spt3) mapped precisely

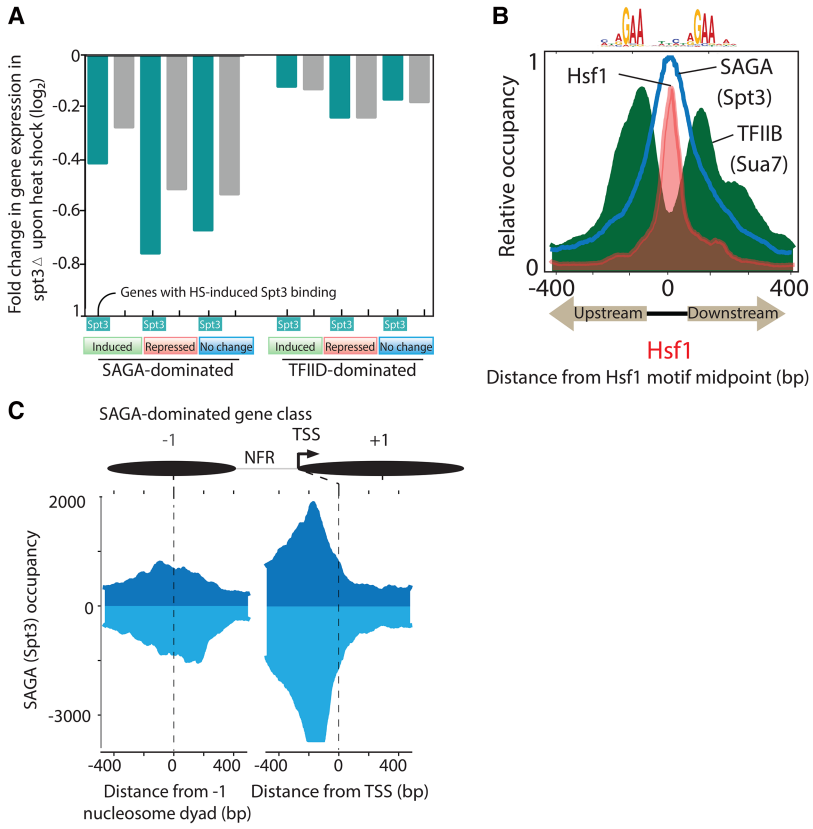

Figure 4. Hsf1 and SAGA precisely colocalize between divergent PICs. (*A*) Log_2 changes in gene expression in an *spt3*Δ strain relative to wild type, under acute heat shock conditions (Huisinga and Pugh 2004). Gene classes are separated first by SAGA- vs. TFIID-dominated, then by heat shock-mediated changes in TFIIH occupancy (Induced, Repressed, No change), then by whether Spt3 was induced to bind upon heat shock (≥1.5 fold-change from mock at 3 min of heat shock). (*B*) Gene averaged plots for Hsf1 (red fill), SAGA (Spt3, blue trace), and TFIIB (Sua7, green filled) with respect to Hsf1 motif midpoint. Data were from 3-min heat shock time point. Genes were not oriented, which results in roughly equivalent levels of TFIIB on either side of Hsf1. (*C*) Gene-averaged plot of strand-separated ChIP-exo tag 5′ ends for SAGA (Spt3), distributed around −1 and TSS features. The direction of coding transcription is from *left* to *right*. Plots of tags mapping to the antisense strand are shown inverted. Data from 3 min of heat shock were used.

to Hsf1-bound sites (Fig. 4B), indicating that Spt3 crosslinking to DNA in these promoters may involve Hsf1 interactions. SAGA (Spt3) is likely also recruited by other factors under heat shock and other inducing conditions. There was additional weak positional enrichment of SAGA (Spt3) at −1 nucleosomes (Fig. 4C, left side), although any such interaction might occur indirectly via SAGA's Gcn5 subunit (Hassan et al. 2002). Conceivably, Hsf1-SAGA interactions might promote −1 nucleosomal interactions with SAGA. What is clear from this analysis is that SAGA is not crosslinking through the PIC and thus may not be stably interacting with the core transcription machinery.

Reorganization of RSC binding upon heat shock

RSC (Rsc9) plays a central role in NFR formation (Badis et al. 2008; Parnell et al. 2008; Hartley and Madhani 2009; Lorch et al. 2011, 2014; Krietenstein et al. 2016). We found RSC (Rsc9) to be generally associated with gene-body nucleosomes under normal growth conditions (Spain et al. 2014), with greater enrichment around −1 and +1 nucleosomes (Fig. 2). A more detailed examination of sense versus antisense strands of the RSC (Rsc9) ChIP-exo data revealed an offset of peaks by ~75 bp that were centered over each nucleosome (semi-transparent purple-filled plots in Fig. 5A). This is consistent with RSC binding and engulfing nucleosomes that flank NFRs (Leschziner et al. 2007). Indeed, the peak of exonuclease stop sites resided 35–40 bp from nucleosome dyads under non-heat shock conditions (Fig. 5A). Since its binding was widespread across most genes and unlinked to transcription (Fig. 3), this interaction may reflect a general NFR maintenance mode that occurs independent of transcription.

Upon acute heat shock, RSC (Rsc9) became enriched in promoter NFRs, ~135 bp upstream of +1 dyads (Figs. 2, 5A). Similar heat shock-induced shifts were observed with other RSC subunits, like Rsc3, Rsc58, and Rsc1 (Supplemental Fig. S6A). However, the effect was diminished but not entirely eliminated with Rsc6 and Sth1 subunits. Thus, there is substantial heat shock-induced reorganization of RSC binding that is manifested through some but not all of its subunits. New interactions may be taking place without necessarily losing old ones.

The NFR-enrichment of RSC (Rsc9) was transient, reaching a maximum intensity by 9 min post-heat shock, then retreating by 15 min (Fig. 5B). The timing was much slower than the reorganization of the GTFs and SAGA, which peaked within 3 min. RSC enrichment in NFRs is of interest because NFRs, by our operational definition, lack nucleosomes (even "fragile" ones) and thus lack what RSC is expected to bind to. Nonetheless, promoters are enriched with CGCG elements and poly(dA:dT) tracts, with which RSC interacts (Supplemental Fig. S6B; Lorch et al. 2014; Kubik et al. 2015; Krietenstein et al. 2016).

Similar and distinct genome-wide positional organization of FACT, Pol II, and nucleosomes

When the histone chaperone and transcription elongation factor FACT (Spt16) and Pol II were examined, both largely tracked together, as expected of FACT's role in chromatin reassembly in the wake of Pol II transcription (Fig. 2; Orphanides et al. 1999; Mason and Struhl 2003; Hsieh et al. 2013). There were two general exceptions. First, FACT (Spt16) did not accumulate beyond the site where the mature transcript ends, in comparison to what is seen for Pol II (Fig. 2, right edge of "bell" for Pol II). Therefore, FACT may disengage from the transcription process before termination. Indeed, it appears to disengage where the terminal genic nucleosome resides. Second, a gene-averaged view showed that FACT (Spt16) and Pol II were not entirely coincident in their gene body peaks of enrichment (Fig. 6A). The most 5′ peak of FACT (Spt16) was ~120 bp downstream from the most 5′ peak of Pol II at the TSS. This suggests that FACT associates with Pol II-

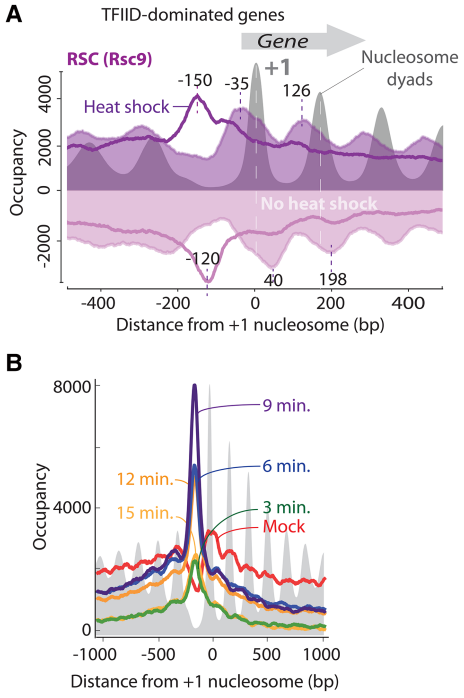

Figure 5. RSC (Rsc9) relocates from gene bodies to promoters upon heat shock. (*A*) Averaged distribution of Rsc9 (normalized unshifted strand-separated tag 5′ ends) plotted with respect to +1 nucleosome dyads at all TFIID-dominated mRNA genes ($n = 4260$). Transcription is oriented to the *right*. ChIP-exo tags mapping to the antisense strand are inverted. Semitransparent purple filled plots represent mock heat shock, and dark purple traces represent acute heat shock (37°C for 3 min). Gray filled plots correspond to nucleosome dyads prior to heat shock which do not change in this bulk assessment upon heat shock. RSC peak distances (in bp) from the +1 dyad are indicated. (*B*) RSC (Rsc9) gene-averaged distribution of normalized shifted tags mapped with respect to +1 nucleosome dyad showing occupancy during mock heat shock (red trace), and a time course of acute heat shock (37°C) for 3, 6, 9, 12, and 15 min in green, blue, magenta, orange, and dark orange traces, respectively. Nucleosome dyads are shown in gray fill.

transcribed regions at a fixed location downstream from where initiation begins. This peak was located ~41 bp downstream from +1 nucleosome dyads and coincided with a second peak of Pol II. Their copositioning might reflect a transient pause of Pol II just beyond the +1 nucleosome dyad where FACT loads. Whether FACT is loading onto nucleosomes or Pol II is not evident from the data.

Under normal (non-heat shock) growth conditions, Pol II and FACT displayed periodic enrichment profiles along gene bodies that possess the same periodicity as nucleosomes (Fig. 6A). We surmise that Pol II dwells longer as it transits the first half of each genic nucleosome, as reported elsewhere in *Drosophila* (Weber et al. 2014), thereby giving it and FACT more opportunity to crosslink there. The periodicity of FACT crosslinking places it positionally just ahead of the periodicity of Pol II crosslinking, which may reflect its location within the elongating complex. However, since FACT is a histone chaperone, it may instead be crosslinking to DNA as an integral part of partially assembled nucleosomes. At the highly expressed RP genes, where few intact nucleosomes remain, the very high relative enrichment of FACT indicates that it may be crosslinking through the transcription machinery, at least at these genes, rather than through nucleosomes. Alternatively, the nucleosomes may be in a highly disassembled state, which are not readily detected by standard MNase-based mapping of nucleosomes.

Upon heat shock, FACT largely relocated to induced genes in lock-step with Pol II (Figs. 2, 3), but neither complex maintained its positional relationships with intact nucleosomes at these genes (Fig. 6B). This might suggest that FACT crosslinks as part of the elongation complex rather than integral to nucleosomes, although this latter possibility is not excluded if nucleosomes become de-localized and/or partially disassembled when highly transcribed (Kireeva et al. 2002; Koerber et al. 2009).

Accumulation of Pol II at the +1 nucleosome region upon heat shock

Under normal growth, Pol II assembles into a PIC at promoters. It rapidly proceeds into an elongating polymerase (Jeronimo and Robert 2014; Wong et al. 2014). Despite its rapid departure at promoters, it dwells there long enough to be detected (Rhee and Pugh 2012). Importantly, none of the GTFs detectably travel with Pol II, including TFIIE, TFIIF, and TFIIH, which appear to remain behind at the promoter (Rhee and Pugh 2012).

Upon acute heat shock, Pol II rapidly accumulated over the +1 nucleosome region of genes and CUTs (but not SUTs or XUTs) (Fig. 2), in comparison to gene bodies (Fig. 3). This occurred regardless of gene expression levels that existed prior to heat shock, or whether the gene was repressed, induced, or unaffected by heat shock (e.g., Rpb3 in Supplemental Fig. S3A).

GTFs produce a characteristic pattern of exonuclease stop sites in the ChIP-exo assay (exemplified by TBP/Spt15 in

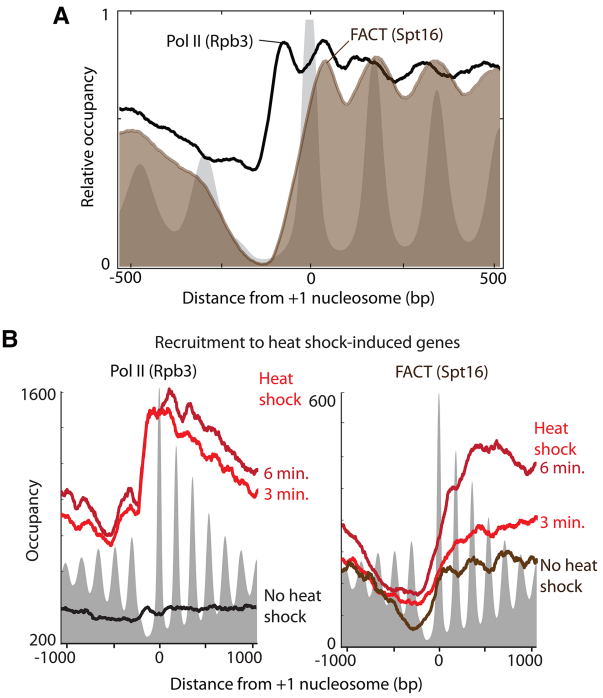

Figure 6. Relocation of FACT upon heat shock. (*A*) Frequency distribution of gene-averaged ChIP-exo tag 5′ ends for Pol II (Rpb3, black trace) and FACT (Spt16, brown fill). Gray filled plots correspond to nucleosome dyads. Coding transcription is oriented to the *right*. Plots are separately scaled to 1 for each data set. (*B*) The absolute occupancy (normalized tag 5′ ends) of Pol II (Rpb3) (*left* panel) and FACT (Spt16) (*right* panel) were averaged at heat shock-induced genes (as defined by increased TFIIH occupancy).

Supplemental Fig. S7A; Rhee and Pugh 2012). This patterning did not change upon heat shock, which implies that GTF organization remained essentially unchanged whether or not Pol II accumulated in the region. This is also where DNA melting occurs upon open complex formation. Therefore, we examined melted PIC DNA to discern whether the accumulated Pol II affected the distribution of single-stranded DNA.

DNA melting within PICs is best assayed in vivo through the selective reactivity of unstacked bases with permanganate (Giardina et al. 1992). This single-nucleotide resolution assay has recently been adopted on a genomic scale (PIP-seq) in flies and humans (Li et al. 2013; Lai and Pugh 2017) but not previously in yeast. We therefore present the first genome-wide measurement of PIC "bubbles" in yeast. Permanganate reacts with T nucleotides in unstacked or melted DNA, and then piperidine is used to cleave the DNA backbone just 3′ to the reacted T nucleotide. Cleavage sites are detected by deep sequencing and marked in the genome when they map immediately 3′ to a T nucleotide (Supplemental Fig. S7B). To ensure that we were examining PICs, rather than elongating Pol II, we performed TFIIB PIP-seq. Immunoprecipitation of TFIIB ensured that any open DNA was associated with TFIIB (i.e., the PIC) at the promoter, in accordance with biochemical and structural observations showing that TFIIB innervates into the Pol II active site within the open promoter DNA but then is dislodged by nascent RNA during transcription elongation (Chen and Hahn 2004; Kostrewa et al. 2009).

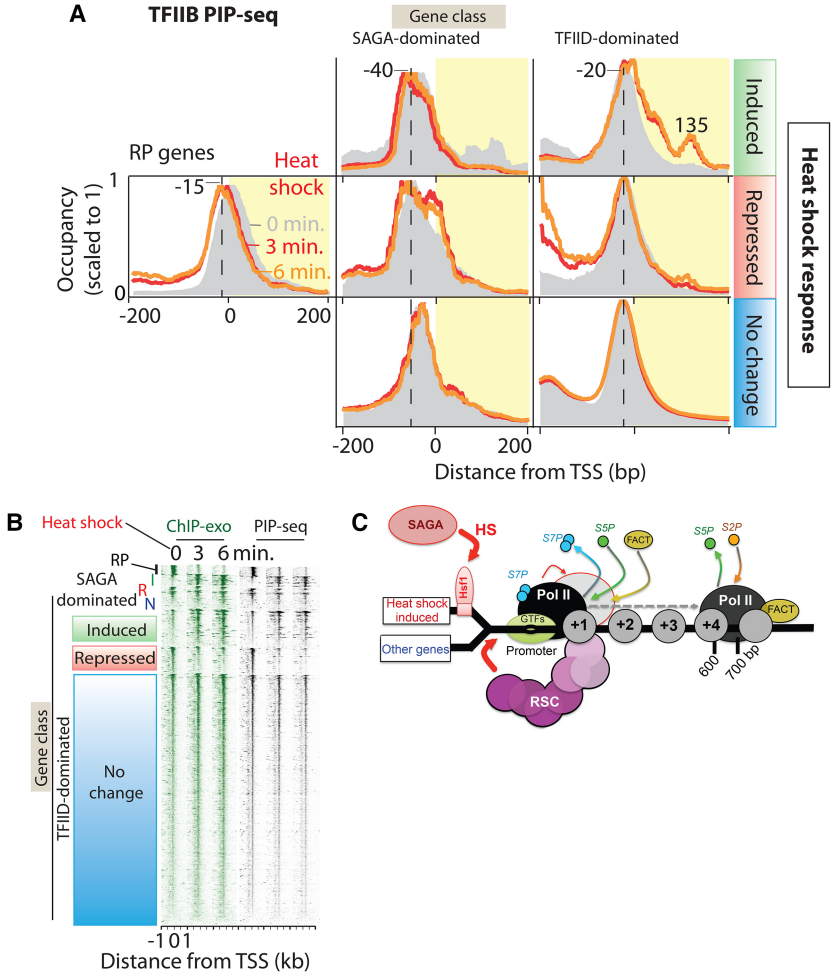

Figure 7. Melted PIC DNA is unaffected by Pol II accumulation in promoter regions. (*A*) Gene-averaged plot of TFIIB PIP-seq tag 5′ ends separated by gene class and heat shock response (i.e., changes in TFIIH occupancy). Mock, 3-, 6-min time points are indicated (gray fill, red trace, orange trace, respectively). Transcription is oriented to the *right*. Plots are scaled to 1. Transcribed regions have a yellow backdrop. Dashed line indicates position of transcription bubble upon heat shock. (*B*) Heat maps of TFIIB (Sua7) ChIP-exo (green), and PIP-seq (black) at 0, 3, and 6 min of heat shock. Gene classes are as in *A*. (*C*) Model for heat shock-induced reorganization of factors at most genes whose expression does not change, and genes whose expression is heat shock-induced.

Under normal growth conditions, open PIC DNA (PIP-seq peaks) was detected ~40 bp upstream of SAGA-dominated TSSs and ~20 bp upstream of TFIID-dominated TSSs (Fig. 7A). This is ~25–30 bp downstream from TATA and TATA-like elements in both gene classes, as reported for individual genes (Giardina and Lis 1993). Thus, stable DNA melting occurs adjacent to the TATA element, rather than at the TSS. From there, as other studies suggest, Pol II scans the DNA to establish a TSS further downstream from the site of stable melting (Kuehner and Brow 2006).

Consistent with lowly expressed genes containing detectable PICs, we detected melted PIC DNA at the vast majority of genes (Fig. 7B). This included heat shock-induced changes in melted DNA that were commensurate with changes in PIC (TFIIH/Ssl2) occupancy. Upon heat shock, the relative levels of melted promoter DNA (TFIIB PIP-seq) matched precisely with PIC occupancy levels (TFIIB ChIP-exo) (Supplemental Fig. S7C). Thus, promoter DNA was melted to the same relative extent that TFIIB was bound. This contrasts with Pol II, which showed relatively greater accumulation in the +1 nucleosome region upon heat shock (Pol II ChIP-exo, Fig. 3) than what is reflected in the promoter DNA melting (Pol II PIP-seq, Fig. 7B). Our simplest interpretation of this relationship is that heat shock may cause some Pol II to accumulate in the +1 nucleosome vicinity but with it not being in an "open" DNA.

Pol II CTD serine 7 is hyperphosphorylated at promoters

The heat shock-induced accumulation of Pol II at the 5′ end of genes raises the question as to the phosphorylation status of the Pol II C-terminal heptad repeat domain (CTD), which cycles through a variety of phosphorylation states during the course of transcription (Lu et al. 1991; Komarnitsky et al. 2000; Buratowski 2009; Mayer et al. 2010; Tietjen et al. 2010; Bataille et al. 2012; Eick and Geyer 2013; Jeronimo et al. 2013; Harlen and Churchman 2017). In particular, phosphorylation on serine at positions 7 and 5 within the CTD (S7P and S5P) occurs near the 5′

ends of genes and continues across gene bodies but with some tapering. S2P occurs deeper within gene bodies, where it remains until the end of the gene. Our high-resolution ChIP-exo data generally support these prior results (Fig. 3; Supplemental Fig. S8). However, we observed a strong spike of S7P at promoters, despite there being only a modest enrichment of Pol II there compared to gene bodies. Thus, the transient nature of Pol II at promoters is accompanied by hyperphosphorylation at S7, followed by its immediate de-phosphorylation upon promoter clearance, although relatively low residual levels of S7P remain across gene bodies. The spike of S7P at promoters was also prominent in the acute heat shock state but did not follow the broader Pol II enrichment that extended across the +1 nucleosome region (Supplemental Fig. S8). The higher resolution and dynamic range of ChIP-exo places a much stronger enrichment of S7P at promoters than has been generally appreciated.

S5P was enriched near the 5′ ends of genes, starting from the TSS. About 600–700 bp downstream, S5P diminished and S2P was enhanced. This represents a more abrupt transition zone than has been previously seen and suggests that S5P de-phosphorylation may be coupled to S2 phosphorylation at a fixed distance downstream from the TSS (but assumes that antibody detection of S5P and S2P are not mutually exclusive). Beyond the transcript end, where Pol II accumulates during termination, high levels of S2P were evident, which is in contrast to recent suggestions (Harlen and Churchman 2017). S2P was also largely absent from ncRNA genes as previously reported (Tietjen et al. 2010). Short genes that terminate before the S5P-S2P transition zone, nevertheless, acquired S2P but only where Pol II accumulated at the two locations at the end of genes: the terminal nucleosome and immediately downstream from the transcript end site.

Discussion

Cells respond to environmental and developmental cues by reprogramming the proteins that interact with the genome, and this results in selective changes in gene expression. The types of involved complexes range from chromatin remodelers to the general transcription machinery to sequence-specific transcriptional regulators. Understanding the role that hundreds, if not thousands, of different proteins play in genome regulation is a substantial undertaking. Our approach has been to inter-relate representatives of different functional classes and characterize their precise positional organization across the yeast genome. We further examine changes that result from near instantaneous reprogramming, such as that arising from heat shock. This allows the temporal plasticity of reprogramming and their structural changes to be examined. Protein–genome interactions are capable of responding within minutes when sensing an environmental signal. For example, within 3 min of heat shock, much of the reprogramming is complete. This attests to the rapidity with which molecular events take place. We find two general reorganization events: (1) global, occurring broadly and not necessarily tied to gene expression; and (2) gene-specific, which results in gene induction or repression of selected genes. Our observations lead to the following view on genome regulation (Fig. 7C), wherein regulatory proteins have a canonical positional organization with respect to gene starts and ends and with each other.

Under normal growth conditions, RSC resides at −1/+1 nucleosomes of a broad set of coding and noncoding transcription units, where it is assumed to help maintain the NFR. It may be retained at −1/+1 by RSC bromodomain interactions with acetylated histones (Spain et al. 2014). Its function there is to maintain NFRs so that PICs can assemble. −1/+1 enrichment is not linked to gene expression levels. Upon heat shock, at least parts of the RSC complex (Rsc1, Rsc3, Rsc9, and Rsc58) accumulate in NFRs, where CGCG motifs and poly(dA:dT) tract may serve as effectors for nucleosome clearance (Lorch et al. 2014; Kubik et al. 2015; Krietenstein et al. 2016). In doing so, RSC keeps NFRs constitutively nucleosome-free, as previous studies have shown (Badis et al. 2008; Parnell et al. 2008; Hartley and Madhani 2009).

Under normal growth conditions (YPD, 25°C), SAGA sparsely occupies promoters in our assay. However, SAGA rapidly and robustly associates with regions upstream of promoters in response to heat shock. These promoters tend to be SAGA-dominated in their regulation, but many others (although proportionally less) have TFIID-dominated regulation. This fits with our previous studies demonstrating that SAGA and TFIID coregulate most genes (Huisinga and Pugh 2004; Ghosh and Pugh 2011). These two classes speak to the relative emphasis of SAGA versus TFIID regulation, rather than being mutually exclusive. SAGA not only associates with stress-induced genes but also associates with promoters that are repressed or unaffected by stress, although proportionally to a lesser extent. This suggests that SAGA might also be linked to other genomic reprogramming events that are not necessarily tied to immediate gene induction. Upon heat shock, a subset of SAGA binding events have maximal positioning where Hsf1 binds its cognate site, more or less constitutively. Since SAGA is also activated to bind promoters that lack Hsf1 binding, there likely exist other Hsf1-independent recruitment mechanisms. However, no other DNA motifs were enriched within these SAGA locations, making it unclear as to its source of promoter specificity. SAGA may use its Spt3 and/or Spt8 subunit to promote Spt15/TBP binding to the TATA core promoter (Eisenmann et al. 1992; Sermwittayawong and Tan 2006). This results in higher levels of GTFs binding to the core promoter, along with Pol II and elevated transcription.

We find that the vast majority of yeast coding and noncoding transcription units have a sufficient basal level of expression such that precisely positioned PICs can be detected above background. In addition, GTFs increase or decrease in occupancy in general accordance with gene induction and repression, respectively. The level of open/melted promoter (as measured here by PIP-seq) complex waxes and wanes accordingly. Pol II also follows this occupancy trend. However, upon heat shock, Pol II tends to accumulate in the +1 nucleosome region of genes whether they are induced, repressed, or unaffected by heat shock. This occurs outside of the PIC region and thus appears to have little impact on measured events at the PIC (GTF binding, promoter melting, Pol II S7P).

Prior biochemical studies suggest that a Pol II having a dephosphorylated CTD is recruited to promoters (Lu et al. 1991). With this assumption, our studies indicate that the arrival of Pol II at promoters under normal conditions rapidly converts its CTD to a S7P state that is associated with the melted promoter complex. Immediately upon promoter escape, S7P is mostly dephosphorylated and S5 of the CTD is phosphorylated. As transcription proceeds through the +1 nucleosome, the histone chaperone FACT associates with Pol II, which may help return nucleosomes within gene bodies. Nucleosomes may impede Pol II transit, thereby creating periodicities in Pol II and FACT positioning that match nucleosome positioning. S5P is maintained for 600–700 bp, rather than for a fixed percentage of gene length, as is commonly depicted. After this point, S5P is mostly de-phosphorylated and S2 is phosphorylated. Genes that are too short to contain the transition

zone nevertheless acquire S2P where Pol II terminates transcription. FACT is largely absent from the site of termination.

Taken together, our results add more pieces to the emerging picture of how proteins that interact with the genome coordinate gene regulation, by demonstrating the intrinsic positional organization of regulatory proteins around genes, and how selected factors are either recruited or repositioned when the genome is reprogrammed. Our findings emphasize the value of examining events that are not necessarily tied to changes in gene expression. The positional reorganization of factors within the same gene may not be observable with lower resolution ChIP-seq assays but instead benefit from assays like ChIP-exo and PIP-seq that have near-base pair positional resolution. Filling in the rest of the puzzle through high-resolution genome-wide studies should provide deeper molecular mechanistic insights into how chromatin and the transcription machinery mutually regulate each other.

Methods

A detailed description of the methods can be found in Supplemental Material as Supplemental Methods. In brief, TAP-tagged strains of *Saccharomyces cerevisiae* were grown in yeast peptone dextrose (YPD) media at 25°C to an $OD_{600} = 0.8$. Cultures were heat-shocked (mock-shocked) by the addition of hot media to achieve a final temperature of 37°C. Incubations were continued for indicated times. Prechilled formaldehyde was added to achieve a final concentration of 1% and final temperature of 25°C. Reactions were quenched and cells collected by centrifugation. For PIP-seq, cells were further incubated in 100 mM $KMnO_4$. For ChIP-exo and PIP-seq, solubilized sonicated chromatin was prepared from bead-beaten cell extracts to achieve a DNA fragment size of <500 bp. For mapping nucleosomes, MNase was applied instead of sonication. Extracts were incubated with IgG antibodies coupled to protein A sepharose. For ChIP-exo, washed immobilized DNA was trimmed in the 5′-3′ direction with lambda exonuclease, until stopped by formaldehyde crosslink. For PIP-seq, the immobilized DNA was treated with piperidine to cleave at permanganate-trapped melted "T" nucleotides. The resulting DNA was subjected to deep sequencing. Data sets used for individual figure panels are indicated in Supplemental Methods. To normalize data sets, each coordinate-strand was rank-ordered within each data set by tag count, then averaged across data sets for each rank order (Qiu et al. 2013). DESeq (Anders and Huber 2010) was used to compute the significant changes in TFIIH (Ssl2) ChIP-exo tag counts upon heat shock in the interval −100 bp to +100 bp from annotated TSSs. Reference +1 nucleosome dyads were from Zhang et al. (2011); TSS locations were from Xu et al. (2009). The set of SAGA/TFIID-dominated genes were obtained from Huisinga and Pugh (2004).

Data access

Sequencing data from this study have been submitted to the NCBI Gene Expression Omnibus (GEO; http://www.ncbi.nlm.nih.gov/geo/) under accession number GSE98573. Scripts and reference files are available at https://github.com/seqcode/vinayachandran_2017_figs, and in Supplemental Methods.

Competing interest statement

B.F.P. has a financial interest in Peconic, LLC, which uses the ChIP-exo technology implemented in this study and could potentially benefit from the outcomes of this research.

Acknowledgments

We thank David Rocco for help in growing and processing the RSC strains, Nina Farrell and Kylie Bocklund for library sequencing, and William Lai and Yunfei Li for bioinformatics support. This work was supported by National Institutes of Health grants GM059055 and ES013768 to B.F.P.

Author contributions: V.V. designed and conducted most experiments and contributed to manuscript writing. R.R. analyzed most of the data. B.P. managed the data and conducted analysis. M.J.R. conducted and analyzed experiments in Supplemental Figure S6 and provided guidance on data analysis. L.R. ensured that analyses were computationally reproducible and accessible on GitHub. C.M. conducted and analyzed experiments in Supplemental Figure S5. S.M. provided supervision, guidance, and support to L.R. B.F.P. conceptualized and supervised the project and wrote the manuscript.

References

Anandhakumar J, Moustafa YW, Chowdhary S, Kainth AS, Gross DS. 2016. Evidence for multiple mediator complexes in yeast independently recruited by activated heat shock factor. *Mol Cell Biol* **36:** 1943–1960.

Anders S, Huber W. 2010. Differential expression analysis for sequence count data. *Genome Biol* **11:** R106.

Badis G, Chan ET, van Bakel H, Pena-Castillo L, Tillo D, Tsui K, Carlson CD, Gossett AJ, Hasinoff MJ, Warren CL, et al. 2008. A library of yeast transcription factor motifs reveals a widespread function for Rsc3 in targeting nucleosome exclusion at promoters. *Mol Cell* **32:** 878–887.

Bailey TL, Elkan C. 1994. Fitting a mixture model by expectation maximization to discover motifs in biopolymers. In *Proceedings of the second international conference on intelligent systems for molecular biology*, pp. 28–36. AAAI Press, Menlo Park, CA.

Baptista T, Grunberg S, Minoungou N, Koster MJE, Timmers HTM, Hahn S, Devys D, Tora L. 2017. SAGA is a general cofactor for RNA polymerase II transcription. *Mol Cell* **68:** 130–143.e135.

Bataille AR, Jeronimo C, Jacques PE, Laramee L, Fortin ME, Forest A, Bergeron M, Hanes SD, Robert F. 2012. A universal RNA polymerase II CTD cycle is orchestrated by complex interplays between kinase, phosphatase, and isomerase enzymes along genes. *Mol Cell* **45:** 158–170.

Berry DB, Gasch AP. 2008. Stress-activated genomic expression changes serve a preparative role for impending stress in yeast. *Mol Biol Cell* **19:** 4580–4587.

Buratowski S. 2009. Progression through the RNA polymerase II CTD cycle. *Mol Cell* **36:** 541–546.

Causton HC, Ren B, Koh SS, Harbison CT, Kanin E, Jennings EG, Lee TI, True HL, Lander ES, Young RA. 2001. Remodeling of yeast genome expression in response to environmental changes. *Mol Biol Cell* **12:** 323–337.

Chen HT, Hahn S. 2004. Mapping the location of TFIIB within the RNA polymerase II transcription preinitiation complex: a model for the structure of the PIC. *Cell* **119:** 169–180.

de Jonge WJ, O'Duibhir E, Lijnzaad P, van Leenen D, Groot Koerkamp MJ, Kemmeren P, Holstege FC. 2017. Molecular mechanisms that distinguish TFIID housekeeping from regulatable SAGA promoters. *EMBO J* **36:** 274–290.

Downey M, Knight B, Vashisht AA, Seller CA, Wohlschlegel JA, Shore D, Toczyski DP. 2013. Gcn5 and sirtuins regulate acetylation of the ribosomal protein transcription factor Ifh1. *Curr Biol* **23:** 1638–1648.

Eick D, Geyer M. 2013. The RNA polymerase II carboxy-terminal domain (CTD) code. *Chem Rev* **113:** 8456–8490.

Eisenmann DM, Arndt KM, Ricupero SL, Rooney JW, Winston F. 1992. SPT3 interacts with TFIID to allow normal transcription in *Saccharomyces cerevisiae*. *Genes Dev* **6:** 1319–1331.

Gasch AP, Spellman PT, Kao CM, Carmel-Harel O, Eisen MB, Storz G, Botstein D, Brown PO. 2000. Genomic expression programs in the response of yeast cells to environmental changes. *Mol Biol Cell* **11:** 4241–4257.

Ghosh S, Pugh BF. 2011. Sequential recruitment of SAGA and TFIID in a genomic response to DNA damage in *Saccharomyces cerevisiae*. *Mol Cell Biol* **31:** 190–202.

Giardina C, Lis JT. 1993. DNA melting on yeast RNA polymerase II promoters. *Science* **261:** 759–762.

Giardina C, Perez-Riba M, Lis JT. 1992. Promoter melting and TFIID complexes on *Drosophila* genes in vivo. *Genes Dev* **6:** 2190–2200.

Hahn JS, Hu Z, Thiele DJ, Iyer VR. 2004. Genome-wide analysis of the biology of stress responses through heat shock transcription factor. *Mol Cell Biol* **24:** 5249–5256.
Harlen KM, Churchman LS. 2017. The code and beyond: transcription regulation by the RNA polymerase II carboxy-terminal domain. *Nat Rev Mol Cell Biol* **18:** 263–273.
Hartley PD, Madhani HD. 2009. Mechanisms that specify promoter nucleosome location and identity. *Cell* **137:** 445–458.
Hassan AH, Prochasson P, Neely KE, Galasinski SC, Chandy M, Carrozza MJ, Workman JL. 2002. Function and selectivity of bromodomains in anchoring chromatin-modifying complexes to promoter nucleosomes. *Cell* **111:** 369–379.
Hsieh FK, Kulaeva OI, Patel SS, Dyer PN, Luger K, Reinberg D, Studitsky VM. 2013. Histone chaperone FACT action during transcription through chromatin by RNA polymerase II. *Proc Natl Acad Sci* **110:** 7654–7659.
Huisinga KL, Pugh BF. 2004. A genome-wide housekeeping role for TFIID and a highly regulated stress-related role for SAGA in *Saccharomyces cerevisiae*. *Mol Cell* **13:** 573–585.
Jakobsen BK, Pelham HR. 1988. Constitutive binding of yeast heat shock factor to DNA in vivo. *Mol Cell Biol* **8:** 5040–5042.
Jansen A, van der Zande E, Meert W, Fink GR, Verstrepen KJ. 2012. Distal chromatin structure influences local nucleosome positions and gene expression. *Nucleic Acids Res* **40:** 3870–3885.
Jeronimo C, Robert F. 2014. Kin28 regulates the transient association of Mediator with core promoters. *Nat Struct Mol Biol* **21:** 449–455.
Jeronimo C, Bataille AR, Robert F. 2013. The writers, readers, and functions of the RNA polymerase II C-terminal domain code. *Chem Rev* **113:** 8491–8522.
Kireeva ML, Walter W, Tchernajenko V, Bondarenko V, Kashlev M, Studitsky VM. 2002. Nucleosome remodeling induced by RNA polymerase II: loss of the H2A/H2B dimer during transcription. *Mol Cell* **9:** 541–552.
Koerber RT, Rhee HS, Jiang C, Pugh BF. 2009. Interaction of transcriptional regulators with specific nucleosomes across the *Saccharomyces* genome. *Mol Cell* **35:** 889–902.
Komarnitsky P, Cho EJ, Buratowski S. 2000. Different phosphorylated forms of RNA polymerase II and associated mRNA processing factors during transcription. *Genes Dev* **14:** 2452–2460.
Kostrewa D, Zeller ME, Armache KJ, Seizl M, Leike K, Thomm M, Cramer P. 2009. RNA polymerase II-TFIIB structure and mechanism of transcription initiation. *Nature* **462:** 323–330.
Krietenstein N, Wal M, Watanabe S, Park B, Peterson CL, Pugh BF, Korber P. 2016. Genomic nucleosome organization reconstituted with pure proteins. *Cell* **167:** 709–721.e712.
Kubik S, Bruzzone MJ, Jacquet P, Falcone JL, Rougemont J, Shore D. 2015. Nucleosome stability distinguishes two different promoter types at all protein-coding genes in yeast. *Mol Cell* **60:** 422–434.
Kuehner JN, Brow DA. 2006. Quantitative analysis of *in vivo* initiator selection by yeast RNA polymerase II supports a scanning model. *J Biol Chem* **281:** 14119–14128.
Kuras L, Kosa P, Mencia M, Struhl K. 2000. TAF-containing and TAF-independent forms of transcriptionally active TBP in vivo. *Science* **288:** 1244–1248.
Lai WK, Pugh BF. 2017. Genome-wide uniformity of human 'open' pre-initiation complexes. *Genome Res* **27:** 15–26.
Lee TI, Causton HC, Holstege FC, Shen WC, Hannett N, Jennings EG, Winston F, Green MR, Young RA. 2000. Redundant roles for the TFIID and SAGA complexes in global transcription. *Nature* **405:** 701–704.
Leschziner AE, Saha A, Wittmeyer J, Zhang Y, Bustamante C, Cairns BR, Nogales E. 2007. Conformational flexibility in the chromatin remodeler RSC observed by electron microscopy and the orthogonal tilt reconstruction method. *Proc Natl Acad Sci* **104:** 4913–4918.
Li J, Liu Y, Rhee HS, Ghosh SK, Bai L, Pugh BF, Gilmour DS. 2013. Kinetic competition between elongation rate and binding of NELF controls promoter-proximal pausing. *Mol Cell* **50:** 711–722.
Lorch Y, Griesenbeck J, Boeger H, Maier-Davis B, Kornberg RD. 2011. Selective removal of promoter nucleosomes by the RSC chromatin-remodeling complex. *Nat Struct Mol Biol* **18:** 881–885.
Lorch Y, Maier-Davis B, Kornberg RD. 2014. Role of DNA sequence in chromatin remodeling and the formation of nucleosome-free regions. *Genes Dev* **28:** 2492–2497.
Lu H, Flores O, Weinmann R, Reinberg D. 1991. The nonphosphorylated form of RNA polymerase II preferentially associates with the preinitiation complex. *Proc Natl Acad Sci* **88:** 10004–10008.
Mason PB, Struhl K. 2003. The FACT complex travels with elongating RNA polymerase II and is important for the fidelity of transcriptional initiation in vivo. *Mol Cell Biol* **23:** 8323–8333.
Mayer A, Lidschreiber M, Siebert M, Leike K, Soding J, Cramer P. 2010. Uniform transitions of the general RNA polymerase II transcription complex. *Nat Struct Mol Biol* **17:** 1272–1278.
Orphanides G, Wu WH, Lane WS, Hampsey M, Reinberg D. 1999. The chromatin-specific transcription elongation factor FACT comprises human SPT16 and SSRP1 proteins. *Nature* **400:** 284–288.
Parnell TJ, Huff JT, Cairns BR. 2008. RSC regulates nucleosome positioning at Pol II genes and density at Pol III genes. *EMBO J* **27:** 100–110.
Qiu X, Wu H, Hu R. 2013. The impact of quantile and rank normalization procedures on the testing power of gene differential expression analysis. *BMC Bioinformatics* **14:** 124.
Radman-Livaja M, Rando OJ. 2010. Nucleosome positioning: How is it established, and why does it matter? *Dev Biol* **339:** 258–266.
Reja R, Vinayachandran V, Ghosh S, Pugh BF. 2015. Molecular mechanisms of ribosomal protein gene coregulation. *Genes Dev* **29:** 1942–1954.
Rhee HS, Pugh BF. 2011. Comprehensive genome-wide protein-DNA interactions detected at single-nucleotide resolution. *Cell* **147:** 1408–1419.
Rhee HS, Pugh BF. 2012. Genome-wide structure and organization of eukaryotic pre-initiation complexes. *Nature* **483:** 295–301.
Sermwittayawong D, Tan S. 2006. SAGA binds TBP via its Spt8 subunit in competition with DNA: implications for TBP recruitment. *EMBO J* **25:** 3791–3800.
Shivaswamy S, Iyer VR. 2008. Stress-dependent dynamics of global chromatin remodeling in yeast: dual role for SWI/SNF in the heat shock stress response. *Mol Cell Biol* **28:** 2221–2234.
Shivaswamy S, Bhinge A, Zhao Y, Jones S, Hirst M, Iyer VR. 2008. Dynamic remodeling of individual nucleosomes across a eukaryotic genome in response to transcriptional perturbation. *PLoS Biol* **6:** e65.
Spain MM, Ansari SA, Pathak R, Palumbo MJ, Morse RH, Govind CK. 2014. The RSC complex localizes to coding sequences to regulate Pol II and histone occupancy. *Mol Cell* **56:** 653–666.
Tietjen JR, Zhang DW, Rodriguez-Molina JB, White BE, Akhtar MS, Heidemann M, Li X, Chapman RD, Shokat K, Keles S, et al. 2010. Chemical-genomic dissection of the CTD code. *Nat Struct Mol Biol* **17:** 1154–1161.
Venters BJ, Pugh BF. 2009. A canonical promoter organization of the transcription machinery and its regulators in the *Saccharomyces* genome. *Genome Res* **19:** 360–371.
Venters BJ, Wachi S, Mavrich TN, Andersen BE, Jena P, Sinnamon AJ, Jain P, Rolleri NS, Jiang C, Hemeryck-Walsh C, et al. 2011. A comprehensive genomic binding map of gene and chromatin regulatory proteins in *Saccharomyces*. *Mol Cell* **41:** 480–492.
Verghese J, Abrams J, Wang Y, Morano KA. 2012. Biology of the heat shock response and protein chaperones: budding yeast (*Saccharomyces cerevisiae*) as a model system. *Microbiol Mol Biol Rev* **76:** 115–158.
Weber CM, Ramachandran S, Henikoff S. 2014. Nucleosomes are context-specific, H2A.Z-modulated barriers to RNA polymerase. *Mol Cell* **53:** 819–830.
Weiner A, Hughes A, Yassour M, Rando OJ, Friedman N. 2010. High-resolution nucleosome mapping reveals transcription-dependent promoter packaging. *Genome Res* **20:** 90–100.
Weiner A, Chen HV, Liu CL, Rahat A, Klien A, Soares L, Gudipati M, Pfeffner J, Regev A, Buratowski S, et al. 2012. Systematic dissection of roles for chromatin regulators in a yeast stress response. *PLoS Biol* **10:** e1001369.
Wong KH, Jin Y, Struhl K. 2014. TFIIH phosphorylation of the Pol II CTD stimulates mediator dissociation from the preinitiation complex and promoter escape. *Mol Cell* **54:** 601–612.
Xu Z, Wei W, Gagneur J, Perocchi F, Clauder-Munster S, Camblong J, Guffanti E, Stutz F, Huber W, Steinmetz LM. 2009. Bidirectional promoters generate pervasive transcription in yeast. *Nature* **457:** 1033–1037.
Yassour M, Kaplan T, Fraser HB, Levin JZ, Pfiffner J, Adiconis X, Schroth G, Luo S, Khrebtukova I, Gnirke A, et al. 2009. Ab initio construction of a eukaryotic transcriptome by massively parallel mRNA sequencing. *Proc Natl Acad Sci* **106:** 3264–3269.
Zanton SJ, Pugh BF. 2004. Changes in genomewide occupancy of core transcriptional regulators during heat stress. *Proc Natl Acad Sci* **101:** 16843–16848.
Zanton SJ, Pugh BF. 2006. Full and partial genome-wide assembly and disassembly of the yeast transcription machinery in response to heat shock. *Genes Dev* **20:** 2250–2265.
Zhang Z, Wippo CJ, Wal M, Ward E, Korber P, Pugh BF. 2011. A packing mechanism for nucleosome organization reconstituted across a eukaryotic genome. *Science* **332:** 977–980.

Received June 23, 2017; accepted in revised form January 25, 2018.